HHS Public Access

Author manuscript

ACS Appl Bio Mater. Author manuscript; available in PMC 2022 April 08.

Published in final edited form as:

ACS Appl Bio Mater. 2021 December 20; 4(12): 8248–8258. doi:10.1021/acsabm.1c00794.

Preventing *Pseudomonas aeruginosa* biofilms on indwelling catheters by surface-bound enzymes

Dalal Asker[1,2,#], **Tarek S. Awad**[1,#], **Deepa Raju**[3], **Hiram Sanchez**[4], **Ira Lacdao**[3], **Stephanie Gilbert**[3], **Piyanka Sivarajah**[3], **David R. Andes**[4,5], **Donald C. Sheppard**[6,7,8,9], **P. Lynne Howell**[3,10,*], **Benjamin D. Hatton**[1,*]

[1]Department of Materials Science & Engineering, University of Toronto, Toronto, Canada

[2]Food Science & Technology Department, Alexandria University, Alexandria, Egypt

[3]Program in Molecular Medicine, The Hospital for Sick Children, Toronto, Canada

[4]Dept of Medicine, University of Wisconsin, 600 Highland Ave, Madison, WI

[5]Medical Microbiology and Immunology, University of Wisconsin, Madison, WI

[6]Infectious Diseases and Immunity in Global Health Program, Research Institute of the McGill University Health Centre, Montréal, Canada

[7]Department of Microbiology and Immunology, McGill University, Montreal, Canada

[8]Department of Medicine, McGill University, Montreal, Canada

[9]McGill Interdisciplinary Initiative in Infection and Immunity (MI4), Montreal, Canada

[10]Department of Biochemistry, University of Toronto, Toronto, Canada

Abstract

Implanted medical devices such as central venous catheters are highly susceptible to microbial colonization and biofilm formation, and are a major risk factor for nosocomial infections. The opportunistic pathogen *Pseudomonas aeruginosa* uses exopolysaccharides, such as Psl, for both initial surface attachment and biofilm formation. We have previously shown that chemically immobilizing the Psl-specific glycoside hydrolase, $PslG_h$, to a material surface can inhibit *P. aeruginosa* biofilm formation. Herein we show that $PslG_h$ can be uniformly immobilized on the lumen surface of medical-grade, commercial polyethylene, polyurethane, and polydimethylsiloxane (silicone) catheter tubing. We confirmed the surface-bound $PslG_h$ was uniformly distributed along the catheter length and remained active even after storage for 30 days at 4 °C. *P. aeruginosa* colonization and biofilm formation under dynamic flow culture conditions *in vitro* showed a 3-log reduction in the number of bacteria during the first 11 days, and a 2-log

*To whom correspondence should be addressed: P. Lynne Howell howell@sickkids.ca & Benjamin Hatton benjamin.hatton@utoronto.ca.

#These authors contributed equally to this work

Author Contributions: TSA, DA, DR, DCS, PLH and BDH designed the research. TSA performed the enzyme immobilization and surface physical and chemical characterizations. DA performed the microbiology tests and image analysis. DA and TSA performed the *in-vitro* flow culture experiments and analyzed all experimental data. IL, SG and PS prepared and purified $PslG_h$. HS and DRA performed the *in-vivo* testing and SEM imaging. TSA, DA, BDH, DR and PLH wrote the paper. All authors reviewed and approved the final manuscript.

reduction by day 14 for $PslG_h$ modified PE-100 catheters, compared to untreated catheter controls. In an *in vivo* rat infection model, $PslG_h$-modified PE-100 catheters showed ~1.5-log reduction in the colonization of the clinical *P. aeruginosa* ATCC 27853 strain after 24 hours. These results demonstrate the robust ability of surface-bound glycoside hydrolase enzymes to inhibit biofilm formation, and their potential to reduce rates of device-associated infections.

Graphical Abstract

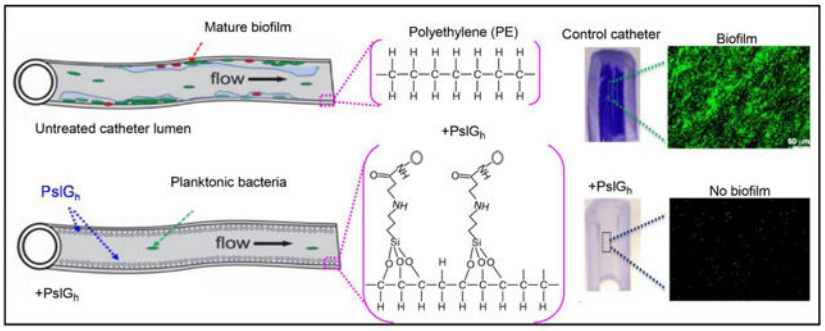

Keywords

catheters; biomaterials; bacterial biofilms; medical device infection; *Pseudomonas aeruginosa* ; enzyme immobilization; glycoside hydrolases; $PslG_h$

1. Introduction

Biofilms formed on implanted medical devices are responsible for 50–70% of all hospital acquired infections, and can be tremendously difficult to treat [1–4]. Biofilms are surface-attached microbial colonies embedded within a self-produced extracellular matrix, composed of exopolysaccharide, extracellular DNA and proteins [5]. Annually, there are an estimated 14 million biofilm infections in the US, causing at least 350,000 deaths [4]. The vast majority of these infections (86–95%) are associated with microbial colonization of catheters *e.g.*, central-line associated bloodstream infections (CLABSI), catheter-associated urinary tract infections (CAUTI), and ventilator-associated pneumonia (VAP) [6–7]. The annual cost of the top five hospital-acquired infections is ~$9.8 billion in the US alone [8]. Indwelling central venous catheters (CVC) are routinely used to administer medications, blood products, and nutritional fluids to patients, for both temporary and long-term use[9]. The clean surfaces of newly-implanted catheters are highly susceptible to microbial colonization [10–13]. The exopolysaccharide component of the matrix impairs antibiotic penetration [14–15] and provides a barrier against phagocytosis by host immune cells [16]. Within biofilms, microbes are up to 1000 times more tolerant to antimicrobials than planktonic cells [1, 10, 17–18]. As a result, device-related biofilm infections are difficult to treat using systemic antibiotics [19], and often require device extraction and replacement.

Medical biofilms can involve a wide variety of organisms, but the bacterium *Pseudomonas aeruginosa* accounts for ~28% of device-related infections [20–23]. *P. aeruginosa* is an ubiquitous, Gram-negative, opportunistic pathogen associated with a wide array of

life-threatening acute and chronic nosocomial infections, particularly in patients with compromised host-defense mechanisms [24]. *P. aeruginosa* infections are becoming more challenging to treat due to the emergence of multidrug resistant strains [14–15, 25–28]. *P. aeruginosa* produces three distinct biofilm exopolysaccharides: Psl, Pel, and alginate [29–31]. The cationic Pel and neutral Psl polysaccharides are produced in varying amounts in different strains [32], while the anionic alginate is synthesized exclusively by mucoid strains in the lungs of cystic fibrosis patients [29–30]. Both Pel and Psl play a significant role in the formation and maintenance of biofilm structure [14, 33], and recent work has shown the role that polysaccharides (such as Psl) play to enable the cell-cell and cell-surface adhesion necessary for biofilm formation [14, 16, 32, 34–35].

Antimicrobial coatings for medical devices often incorporate silver, chlorhexidine, or triclosan for diffusive release [13, 36–38]. These coatings are often ineffective over time as they do not directly prevent microbial attachment, and new cells eventually accumulate on dead cells [39]. Diffusional release is also limited by a number of factors, including: (i) slow diffusion rates to the material surface; (ii) decreased activity over time as the antimicrobial concentration decreases and bacterial biomass accumulates [40]; and (iii) antimicrobial tolerance [41–42]. These limitations have led to an alternative trend to develop non-adhesive, non-fouling surfaces that target the early stages of biofilm development. These materials are designed to keep bacteria in a planktonic (swimming) state [43–45] and thus more susceptible to antibiotics and the host immune system [10]. Non-fouling, 'bio-passive' polymer brush surfaces, such as hydrophilic polyethylene glycol (PEG) are effective, but tend to fail after a period of days [46–47]. Slippery liquid infused porous surfaces (SLIPS) show highly-effective, long term anti-fouling properties but clinical performance is still unclear [48].

Recently, we developed novel 'bioactive' biomaterial surfaces by covalently immobilizing the glycoside hydrolase, $PslG_h$. In solution, this enzyme has been shown to disrupt *P. aeruginosa* biofilms *in vitro* [49–50]. We immobilized $PslG_h$ to flat squares of glass, polydimethylsiloxane (PDMS) and polystyrene (PS), and demonstrated that the surfaces prevented adsorption by hydrolyzing Psl [51]. The $PslG_h$-bound surfaces reduced *P. aeruginosa* biofilms by 3–4 log units (8 d in static culture), compared to controls. However, to be suitable for clinical application, it is important to uniformly immobilize $PslG_h$ along the length of the (inner) lumen surface of medical-grade catheters, and demonstrate long term activity to prevent *P. aeruginosa* biofilm growth. Herein, we show that $PslG_h$ surface-modified catheters of polyethylene (PE), PDMS and polyurethane (PU) not only exhibit significantly reduced rates of biofilm formation under flow culture *in vitro* but also *in vivo* using a rat catheter infection model.

2. Materials and Methods

2.1. Materials

Aminopropyl trimethoxysilane (APTMS), glutaraldehyde (GDA), ethanol (HPLC grade), Fetal bovine serum (FBS) and all other reagents were of high analytical grade and were purchased from Sigma Aldrich (Mississauga, ON). Commercial polyethylene (PE), polyurethane (PUR) and polydimethylsiloxane silicone (PDMS) tubing with identical dimensions (0.3 cm ID and 0.6 cm OD) from McMaster-Carr (Ohio, USA), and medical

grade polyethylene (PE-100) catheters (0.8 mm, ID) (Intramedic, Becton Dickinson and Company, NJ) were used as biomaterial surfaces.

2.2. Strains, media and growth conditions

Strains used in this study are *P. aeruginosa* PAO1 (wild-type strain; serotype O5) and *P. aeruginosa* ATCC 27853 (clinical strain). Lysogeny broth (LB) and agar were used for standard culture conditions. To prepare a pre-culture of tested strains, a single colony of freshly grown bacterial cells grown on LB agar overnight at 37 °C was inoculated in 5 mL LB and incubated at 37 °C overnight with agitation. Bacterial biofilms were grown in LB without salt (LBNS). Serum treatment was performed by coating the catheter segment with 100 μL of FBS then incubating without shaking at room temperature for 30 min.

2.3. Enzyme purification

The hydrolase domain of $PslG_h$ was cloned into an expression plasmid and purified from *E. coli* as previously described [50, 52]. Briefly, the enzyme was recombinantly expressed in *E. coli* cells and grown in autoinduction media overnight at 37 °C with 50 μg/mL kanamycin. The protein was purified by Ni-NTA affinity chromatography using an N-terminal His_6-tag present on the enzyme followed by size exclusion chromatography (HiLoad 16/600 Superdex 200 pg, GE Healthcare). The protein was eluted in 20 mM Tris (pH 7.5), 150 mM NaCl, and 2% (vol/vol) glycerol and stored at −80 °C until required. The His_6-tag was left intact for all experiments.

2.4. Surface modification and enzyme immobilization

Enzyme immobilization by covalent binding for the activated surfaces was performed as previously described [51]. We took advantage of surface hydroxyl or carboxylic groups as reactive sites for the APTMS, creating primary amines to be covalently linked to those of the $PslG_h$ by GDA (Figure 1A). All polymer sheets and tubing (PE, PU and PDMS) and medical grade PE catheters (PE-100) were sonicated in absolute ethanol for 15 min then oven dried. Dried samples were exposed to atmospheric plasma (Harrick Plasma PDC001) at high power for up to 10 min. To ensure an even hydroxylation of the lumen surface, sections were flipped end to end after 5 min then exposed to plasma for additional 5 min. Samples were then functionalized with amine (NH_2) groups by immersion in APTMS (Sigma-Aldrich, 97%) solution (50 mg/mL in 80% (v/v) ethanol) for 2 h with shaking at 25 °C according to a published protocol [53]. Tubing segments were checked for any air bubbles that may prevent the APTMS contact with the lumen. After silanization, the surfaces were washed three times with 80% (v/v) ethanol to remove unreacted APTMS. The amino-functionalized surfaces were then immersed in 2% (v/v) GDA in 1×PBS buffer solution (pH 7.2) for 2 h under gentle stirring at 25 °C. The surfaces were rinsed 3 times with sterile 1× PBS to remove unreacted GDA. Functionalized (NH_2-GDA) surfaces were immersed in $PslG_h$ solution (80 μg/mL in 1x PBS buffer) and incubated overnight at 4 °C then washed several times with 1× PBS buffer to remove the unbound enzyme. The concentration of immobilized enzyme was determined from the difference between the concentration of $PslG_h$ in solution prior to immobilization minus the amount of protein that remained in the solution after the immobilization and washings steps. The enzyme concentration before and

after immobilization and in washing buffers was measured using the Bradford protein assay (B6916, Sigma) with bovine serum albumin as a standard.

2.5. Physical and chemical surface characterization

Surface wettability measurements and attenuated total reflection Fourier transform infrared spectroscopy (ATR-FTIR, PerkinElmer Spectrum 100) were used to monitor each step of the process including the surface activation (hydroxylation), silanization (APTMS), cross linking (GDA), and enzyme covalent binding (correlated with the spectra of native components). After a background scan, spectra were collected from 4000 to 625 cm^{-1} using 64 scans at 4 cm^{-1} resolution. The reflection intensities were corrected to compensate for their frequency (wavenumber) dependence (i.e., neglect the effect of frequency). Surface wettability of 'wide' tubing segments was assessed by measuring the static water contact angle using the sessile drop method. Tubing segments were cut longitudinally into two halves and a 1 μL drop of dH_2O was placed on the lumen surface and imaged. The angle between the horizontal plane and the tangent to the drop at the point of contact with the surface was analyzed by ImageJ [54] using the contact angle plugin [55]. For thin PE-100 catheters, the lumen surface wettability was evaluated by lowering the catheters into identical vials half filled with distilled water and measuring the water level change inside the lumen. To evaluate the surface chemistry of the lumen, tubing was cut longitudinally into small, low curvature segments and the interior surface (lumen) was pressed firmly against the face of the ATR crystal to improve surface contact and obtain high quality absorbance/transmission signals.

2.6. Antibiofilm activity under static culture conditions

PAO1 cells were grown in LB medium at 37 °C overnight with shaking at 200 rpm. Cell cultures were normalized to an $OD_{600\ nm}$ of 0.5 and diluted in LBNS (1:100). 5 mL of the diluted culture was added to sterile 6-well polystyrene microplates (Thermo Scientific cat. no. 243656) containing the tested catheters segments (2.5 cm). The culture plates were incubated for 24 h at 25 °C. After incubation, catheters were removed, drained, and rinsed 3x with 10 ml of sterile 1× PBS buffer (pH 7.2) to remove non-adherent cells and media. Under strict sterile conditions, the catheters were cut into 1 cm segments and transferred to separate sterile vials for Sytox Green, crystal violet (CV) staining and colony forming units (CFU) counts, respectively.

2.7. Antibiofilm activity *in vitro* under dynamic flow conditions

P. aeruginosa PA01 biofilms were grown in a lab-made 'two catheters' device, in which the sterile untreated (control) and $PslG_h$ bound PE-100 (10 cm) were installed together with one inlet and one outlet device (Figure S1). *P. aeruginosa* PAO1 was grown in LB Broth overnight, with shaking at 37 °C. The culture was then diluted 1:100 into 150 mL of fresh LBNS Broth in a 250 mL Erlenmeyer flask and stirred. The device inlet was connected to the inoculated media, and the outlet was connected to a tube mounted into a peristaltic pump (Cole Parmer) head and into a waste media bottle. The experiment began once the inoculated medium started flowing from the end of PE-100 catheters, and the flow was stopped to allow for cell attachment and biofilm growth under static conditions. After 24 h, under aseptic conditions the Erlenmeyer flask was disconnected and 20 L of diluted (1/10) and sterilized

LBNS media in a container was connected to the device and media flow (0.4 mL/min) was started. LBNS media was pumped through the reactor from the top, and the waste was dispensed from the side to ensure removal of all free, unattached cells and allow the attached cells to form biofilms under flow conditions for 14 d. A filtered port was used to provide air to the bacteria. A 1 cm section of each tubing was taken daily under sterile conditions and used in a crystal violet (CV) assay, and for SYTOX Green and CFU measurements. For PE catheters, multiple 10 cm sections of the control and $PslG_h$-bound were connected between two multichannel devices. In this case, after long-term continuous flow (~14 d), a whole catheter was disassembled and cut into sections under sterile conditions for biofilm analysis (CV, fluorescence microcopy and CFU).

2.8. Biofilm inhibition *in vitro* assay

To examine biofilm inhibition using a microtiter plate assay, *P. aeruginosa* strain ATCC27853 was grown at 37 °C overnight with shaking at 200 rpm. The cultures were normalized to an OD_{600} of 0.5 and then diluted 1:100 in LBNS. Diluted culture was added to sterile 96-well polystyrene microtiter plates (Thermo Scientific cat. no. 243656), and varying concentrations of $PslG_h$ (0.1 to 10 μM) were added. The cultures were incubated statically for 24 h at 37 °C to allow for biofilm formation. To eliminate edge effects, ~200 μL of sterile water was placed in all outside wells, and the plate was sealed with parafilm. After incubation, nonadherent cells and media were removed by thoroughly washing the plate with deionized water. The wells were stained with 150 μL of 0.1% (w/v) crystal violet for 10 min and then rinsed with water. The remaining dye was solubilized by addition of 150 μL of 95% (v/v) ethanol and left for 10 min, after which the absorbance was measured at 595 nm using a SpectraMax M2 spectrophotometer (Molecular Devices). The amount of biofilm was proportional to the absorbance from staining with crystal violet. Experiments were performed in triplicate and all statistical analysis were performed using GraphPad Prism.

2.9. Antibiofilm activity *in vivo*

P. aeruginosa ATTC 27853 biofilm formation on coated catheters *in vivo* was evaluated using a rat venous catheter model previously developed to study *Candida albicans* biofilm formation 63. Pathogen-free female Sprague-Dawley rats weighing 400 g (Harlan Sprague-Dawley, Indianapolis, Ind.) were used. Animals were maintained in accordance with the American Association for Accreditation of Laboratory Care criteria, and all studies were approved by the institutional animal care committee. Briefly, 24 h after implantation, the jugular venous catheters (PE-100) were inoculated (10^7 cells/mL) and allowed to dwell for 6 h before washing excess inoculum. Rats were sacrificed after 24 h and the catheters collected for bacterial enumeration or imaging by scanning election microscopy (SEM)[56].

2.10. Cell viability assay

To quantify viable bacteria as colony forming per units (CFU), catheters segments were immersed in 10 mL of 1× PBS, sonicated at low power for 5 min and vortexed for 15 s to release viable cells. Aliquots were diluted 10^2-to10^8-fold, and 100 μL of each dilution was plated in duplicate on LB plates. The number of colonies was counted after incubation at 37 °C for 24 h.

2.11. Fluorescence imaging of attached bacteria and biofilm

After catheter segments were rinsed with 1×PBS at pH 7.2, the adherent bacteria were fixed by 2.5% (v/v) glutaraldehyde (GDA) in 1×PBS solution for at least 1 h, then rinsed 3 times with 1×PBS to remove unreacted GDA. After fixation, samples were treated with Tween-20 (0.05% (v/v) in PBS buffer) for 10 min, rinsed with sterile PBS, and stained in the dark with SYTOX green (Life Technologies, CA, USA) for 30 min [37, 56, 62]. Samples were imaged by fluorescence microscopy (Olympus BX63, Tokyo, Japan) using a 20X dry objective. The green fluorescence of the biofilm was observed through a GFP filter ($\lambda_{ex}/\lambda_{em}$ 395/470 nm). The fluorescence densities of biofilms were quantified using computerized image analysis with Olympus CellSens micro imaging software. Each data point represents the average of six images. Error bars represent standard deviation from the mean ($n = 6$).

2.12. Crystal violet staining of biofilms

Crystal Violet (CV) staining was used to visualize the biofilm biomass on catheters. Briefly, after the catheters were rinsed with 1× PBS buffer and air dried for 1 h at 25 °C, they were stained with 300 μL of 0.5% (w/v) CV for 30 min, then rinsed with dH_2O. CV-stained catheters segments were air dried and photographed.

2.13. Scanning electron microscopy

Catheters segments were rinsed with 1× PBS buffer and placed in fixative (1% (v/v) GDA and 4% (v/v) formaldehyde) overnight. The samples were rinsed in 1× PBS buffer two times and then placed in 1% (v/v) osmium tetroxide for 30 min, followed by immersion in hexamethyldislilazane (Polysciences, Inc., Warrington, Pa.). The samples were subsequently dehydrated in a series of ethanol washes (30% (v/v) for 10 min, 50% for 10 min, 70% for 10 min, 95% for 10 min, and 100% for 10 min). Final desiccation was accomplished by critical-point drying (Tousimis, Rockville, MD). Specimens were mounted on aluminum stubs and sputter coated with gold. Samples were observed in a scanning electron microscope (Hitachi S-5700) in the high-vacuum mode at 10 kV. The images were processed for display by using Adobe Photoshop version 5.0.

3. Results

3.1. Immobilization of $PslG_h$ on polymer tubing by covalent binding

In our previous study, we covalently immobilized $PslG_h$ to flat glass, PDMS and PS squares, to demonstrate that a continuous enzymatic degradation of Psl disrupted *P. aeruginosa* attachment and biofilm formation[51]. Extending this approach to medically relevant devices, we first tested conditions for uniform immobilization of $PslG_h$ to the lumen surface of catheters of reasonable length (>10–20cm), where physical access is difficult. The materials of commercial catheters, PE, PDMS and PU, are useful for their chemical inertness (in addition to low friction coefficient, strength, and sterilizability), but also make them difficult to chemically functionalize.

For $PslG_h$ immobilization, we used a 4-step process: surface hydroxylation by plasma oxidation; amine-functionalization by APTMS; GDA cross-linking and $PslG_h$ covalent binding (Figure 1A)[51]. Surface hydroxylation is the key step in $PslG_h$ immobilization to

generate active sites (e.g. OH and COOH) for APTMS[57]. The plasma treatment time to hydroxylate PE surface was tested first for simple PE sheets (1cm^2), and their surface wettability was evaluated by water contact angle. Treating PE sheets with 5 min plasma exposure significantly reduced the contact angle from 92° ±2 (hydrophobic) to 21° ±1 (hydrophilic) (Figure S2A), indicating an increase in surface polar groups. ATR-FTIR confirmed a weak O-H broad band at ~3400 cm^{-1} (Figure S2B). The low intensity of the O-H signal is due the thin surface layer and the limited sensitivity of ATR-FTIR [57]. For PDMS and PU sheets, atmospheric plasma treatment for 5 min also caused a reduction in contact angle from 108° ±4 and 69° ±2 to 21° ±3 and 20° ±1, respectively.

Tubing segments (0.5 cm, ID) of PE, PDMS and PU were then treated with plasma for 5 min, silanized with APTMS and the $PslG_h$ cross-linked with GDA. The success of chemical immobilization along tubing length was confirmed by ATR-FTIR after each step (Figure 2A–C). ATR-FTIR spectrum of the lumen surface of untreated (control) PE tubing (Figure 2A) showed three ethylene bands at 3000–2800 cm^{-1} (CH_2 asymmetric and symmetric stretching), 1500–1400 cm^1 (1473 and 1463 cm^{-1} bending and wagging deformation at 1366) and 730–720 cm^{-1} (rocking). After plasma treatment, we observed a small O-H broad band centered at ~3400 cm^{-1} of the hydroxyl (OH) groups[56]. Addition of APTMS shows FTIR spectra with peaks belonging to C-H (~2900 cm^{-1}) and N-H (~3300 cm^{-1}) stretching vibrations, and peaks corresponding to hydroxyl groups (~3400 cm^{-1}) and C=O (~1635 cm^{-1}) stretching vibrations after the addition of GDA. After incubating with $PslG_h$, the spectrum showed a signal at 1635 cm^{-1} associated with the carbonyl (C=O) vibrations of an amide I band, and a broad band of O-H and N-H stretching vibrations centered at 3343 cm^{-1}. These signals were similar to those obtained from the IR analysis of pure $PslG_h$ in buffer solution [51]. For PDMS and PU tubing, similar modifications in the surface chemistry were detected by ATR-FTIR (Figure 2B and C) confirming the attachment of $PslG_h$ to these two surfaces. Collectively, these surface characterizations confirm successful covalent immobilization of $PslG_h$ to the lumen surface of PE, PDMS and PU tubing.

3.2. Immobilization of $PslG_h$ on PE-100 microcatheters

After $PslG_h$ immobilization on wide tubing (0.5 cm, ID), we next tested short segments (2.5 cm) of medical grade PE-100 microcatheter (0.8 mm, ID). As shown in Figure 2D, we could measure changes in lumen hydrophobicity by the relative capillary rise of water due to capillary action [58]. The capillary height for the control PE-100 catheters was ~ 1 cm below the water level (Figure 2D) due to its hydrophobic surface. Plasma treatment increased the water level by ~ 2 cm, showing a hydrophilic character. Adding APTMS, the water level decreased below the surface level due to the increased number of hydrophobic C-H and N-H groups on the surface (Figure 2D), while GDA increased the capillary rise again due to the hydrophilic hydroxyl (O-H) and carbonyl (C=O) groups. After $PslG_h$ immobilization, the lumen surface maintained its hydrophilic character.

The average length of a CVC catheter insertion is 11–14 cm [9], so for the *in vitro* and *in vivo*-testing we prepared 14 cm lengths of PE-100 medical grade tubing with $PslG_h$. As the lumen of a longer catheter is not directly exposed inside the plasma treatment chamber, the efficiency of hydroxylation may be affected. To test the uniformity along the

tubing length, the catheters were cut into 4 equal segments after each immobilization step, and their hydrophobicity and surface chemistry measured by capillary rise and ATR-FTIR, respectively. We found that plasma treatments of < 10 min resulted in variations in the level of water reached within each segment (S1-S4) of the lumen, but exposures of 10 min or more resulted in uniform hydroxylation with even capillary rise for all 4 segments (Figure 2E). Importantly, identical water level (indicative of hydrophilicity) (Figure S3A) and ATR-FTIR spectra (indicative of surface chemistry) (Figure S3B) were also observed for all 4 sections after $PslG_h$ immobilization, suggesting that $PslG_h$ was also evenly immobilized along the entire length of these PE-100 catheters.

3.3. $PslG_h$ modified polymer tubing inhibit biofilm formation

We first tested the resistance of covalently-bound $PslG_h$ on PE, PDMS, PU tubing to *P. aeruginosa* PAO1 biofilm formation under static culture conditions. Fluorescence microscopy using SYTOX green was used to visualize attached bacterial cells and biofilm formation after 24 h growth. While dense biofilms were observed on the three untreated controls, those with bound $PslG_h$ showed significantly lower cell attachment and colony formation (Figure 3A). Image analysis (cell count/cm^2) revealed that the bound $PslG_h$ significantly reduced the number of attached cells by at least 2-log (Figure 3B). These results confirm the uniformity of bound $PslG_h$ along the lumen length of PU and PDMS and that the surfaces can effectively inhibit the adhesion, colonization and subsequent biofilm formation of *P. aeruginosa* PAO1.

3.4. $PslG_h$ modified PE-100 microcatheters inhibit biofilm formation

Previously, we found that the enzymatic activity of covalently-bound $PslG_h$ on glass surfaces was dependent on the enzyme surface density[51]. To maximize the immobilized $PslG_h$ surface density on the lumen surface of PE-100 microcatheters, we varied the $PslG_h$ concentration (0, 20, 40, 80 and 160 μg/ml) in the immobilization buffer. The surface density of bound $PslG_h$ was determined from the difference between its concentration before and after immobilization using the Bradford protein assay [51]. The amount of surface-bound $PslG_h$ increased exponentially with increasing $PslG_h$ concentration in the buffer up to a $PslG_h$ concentration of 80 μg/ml, at which point the maximum immobilization capacity is likely reached (Figure 4A). The maximum $PslG_h$ surface density was estimated to be about 1.86 μg/cm^2. Fluorescence microscopy images showed a thick biofilm developed on the lumen surface of short (2.5 cm) untreated PE-100 microcatheter after exposure to *P. aeruginosa* PAO1 under static culture condition for 24 h (Figure 4A). However, a moderate reduction in the biofilm growth was observed even at a low density (1.18 μg/cm^2) of surface-bound $PslG_h$, and complete inhibition of bacterial attachment and biofilm formation was observed at a $PslG_h$ surface density of 1.78 μg/cm^2 and above (Figure 4A).

To ensure that the anti-biofilm activity was due to the bound $PslG_h$ specifically, we tested the effects of surface functionalization with APTMS and GDA on *P. aeruginosa* biofilm formation. The number of bacterial cells attached to APTMS (1.7×10^6 CFU/cm^2) and GDA (2.7×10^6 CFU/cm^2)-treated lumen surfaces after 24 h were not significantly different from that of the untreated microcatheter lumen (2.3×10^6 CFU/cm^2). However, a ~3-log reduction in attached cell numbers was observed with $PslG_h$-immobilized vs untreated microcatheters

(1.7×10^3 vs 2.3×10^6 respectively, Figure 4B). In addition, SYTOX green (SG) and crystal violet (CV) staining demonstrated the formation of thick biofilm on the lumen surface of untreated microcatheters and those treated with APTMS or GDA, while biofilms were absent from the lumen of $PslG_h$-treated PE-100 microcatheters (Figure 4B). Combined, these results demonstrate that the anti-biofilm activity of the PE-100 microcatheters against *P. aeruginosa* is due to the immobilized $PslG_h$ rather than other effects of the immobilization process on the microcatheter lumen surface.

To test the activity of the modified PE-100 microcatheters against clinical strains, we used *P. aeruginosa* strain ATCC 27853, a clinical strain with great ability to produce a more robust biofilm compared to the lab PAO1 strain[59]. We first tested the ability of $PslG_h$ in solution to inhibit its biofilm formation. Our results demonstrate that the $PslG_h$ in solution is effective at inhibiting *P. aeruginosa* ATCC 27853 biofilms with an EC_{50} of ~ 1 nM (Figure S4A). Fluorescence microscopy images of the lumen surface of untreated PE-100 microcatheter showed a thick biofilm after exposure to *P. aeruginosa* ATCC 27853 under static culture condition for 24 h (Figure S4B). However, a significant reduction in the number of attached cells (~3-log) was observed compared to the control (Figure S4C).To ensure the activity of immobilized $PslG_h$ along the entire microcatheter length (10 cm), we tested the anti-biofilm activity against *P. aeruginosa* PAO1 biofilm under 24 h static culture. After incubation, CV staining of biofilm mass along the 10 cm microcatheter showed almost no biofilm formation on the $PslG_h$-bound lumen surface, whereas a heavily CV-stained biofilm appeared within the untreated PE-100 control catheter after 24 h (Figure 5A). To test the uniformity of the anti-biofilm activity along the entire 10 cm catheter lumen, catheters were cut into ten 1-cm long segments after incubation in the same conditions as above. Then, 5 alternating segments (Figure 5B) were tested for resistance to *P. aeruginosa* PAO1 biofilm formation using fluorescence microscopy (S2, S4, S6, S8, S10) and CFU (S1, S3, S5, S7, S9). Microscopic images showed thick biofilms within all 5 segments of the untreated catheter lumen (Figure 5C). In comparison, the covalently-bound $PslG_h$ significantly eliminated biofilm formation of *P. aeruginosa* for all PE-100 segments (Figure 5C). Quantitative culture confirmed that the $PslG_h$-treatment of catheters significantly reduced attached cell density from 6.5–6.8 $\times 10^6$ CFU/cm^2 (untreated control) to 1–8.3 $\times 10^3$ CFU/cm^2 ($PslG_h$-bound) after 24 h, representing a ~3-log reduction in CFU (Figure 5D). These results confirm we succeeded in generating a uniform, high density $PslG_h$ coating of the lumen surface, with strong anti-biofilm activity against *P. aeruginosa* along the length of these medical grade PE-100 catheters.

3.4. *In vitro* flow culture

We next tested the $PslG_h$-modified catheters in an *in vitro* flow culture model (Figure S1). *P. aeruginosa* cells were allowed to adhere under static culture conditions for 1 day after which a constant flow (0.6 mL/min) of fresh LBNS media was passed through the lumen of both untreated control and $PslG_h$-bound PE-100 catheters in parallel. Fluorescence microscopy (Figure 6A) demonstrated that the $PslG_h$-bound catheters were resistant to biofilm formation on the lumen surface for the 14 d test period under dynamic culture flow conditions, as compared to the control PE-100 catheters. The rate of cell attachment and biofilm formation was also measured under these flow culture conditions. Quantitative culture confirmed that

$PslG_h$-bound catheters exhibited an ~ 3 log reduction in attached cell numbers during the first 11 d of flow, as compared to untreated catheters. Bacterial counts for the untreated catheters decreased between days 11 and 14, which resulted in a reduction of only 2 log between the treated and control catheters at day 14 (Figure 6B). Taken together, these results indicated that $PslG_h$ immobilized on the catheter lumen surface inhibits biofilm growth for at least 14 d under dynamic flow culture conditions.

3.5. Antibiofilm activity of $PslG_h$ modified catheter in presence of serum

As a prelude to an *in vivo* study, we investigated the effect of blood proteins, storage stability and catheter sterility on the antibiofilm activity of the $PslG_h$-bound catheters. Immediately after catheterization, the surface of indwelling catheters becomes covered with plasma proteins that could potentially interfere with the function of the immobilized enzyme. Therefore, the activity of the lumen-bound $PslG_h$ was tested after being treated with serum for 24 h. In general, there were significant increases in the number of cells that adhered on both untreated and treated catheters after serum treatment (Figure S4). Nevertheless, CV staining (Figure S4A) and SYTOX green (Figure S4B) both confirmed a reduction in bacterial biofilm biomass on the lumen surface of $PslG_h$-bound catheters relative to the untreated control catheter, despite treatment with serum. A few cell clusters were observed by fluorescence microscopy of the $PslG_h$-bound catheter lumen (Figure S4B). Quantitative culture showed that, relative to the control catheters, immobilized $PslG_h$ reduced attached cell density within the catheter lumen before and after serum treatment by 3-log and ~2.5-log, respectively, (Figure S4C). Our results show that while serum proteins increase the adherence of cells to both the control and enzyme-treated surfaces, the $PslG_h$-bound PE catheters remain more resistant to cell attachment even in the presence of serum.

3.6. Sterility and shelf-life storage of the catheter and $PslG_h$ modified catheter

Immobilization procedure (Figure 1) was carried out under aseptic conditions. Prior to immobilzations, caatheters were either pre-sterilized using70% ethanol or ethylene oxide. The immobilzation steps involve the use of atmospheric plasma, 80% ethanol, 2% GDA and filter sterilized $PslG_h$ in PBS buffer which are sufficient to maintain the sterility of catheters during immobilization. To confirm, we tested the sterility of $PslG_h$-bound catheters with a standard plate counting method. Results confirmed the absence of contamination.

In addition, we tested the storage stability of $PslG_h$-bound catheters after storage for 30 d at 4 °C under both dry and wet conditions. $PslG_h$-bound catheters were found to remain resistant to biofilm formation as shown from fluorescence microscopy (Figure S6A) and their corresponding cell counts, which exhibited a 2.5–3 log reduction (Figure S6B).

3.7. $PslG_h$ modified catheter inhibits biofilm formation *in vivo*

Finally, we tested the anti-biofilm activity of these $PslG_h$-bound PE-100 catheters in the complex environment found *in vivo*, using a central venous catheter infection (biofilm) rat model [65]. In this model, the clinical strain *P. aeruginosa* ATCC 27853 was chosen as it was isolated from a hospital blood specimen and has been shown to produce a more robust biofilm compared to the lab PAO1 strain [59]. Twenty-four hours after intravascular placement, SEM imaging of untreated catheter segments (Figure 7A) showed

a dense biofilm network that consists of a relatively large number of cells enclosed in an extracellular matrix. In comparison, segments from the $PslG_h$-bound catheter contained scattered and weakly attached cells and a lack of biofilm matrix. Quantitative culture of the $PslG_h$-bound catheter showed a significant inhibition of biofilm formation 24 h after infection, as compared to the untreated catheters (~2 log CFU reduction) (Figure 7B).

4. Discussion

Developing robust approaches to limit bacterial biofilm formation on biomaterials through non-fouling (non-biocidal) mechanisms remains relatively new for antimicrobial biomedical devices. Antimicrobial strategies that do rely on biocidal drug release [60] are generally ineffective over time as they cannot prevent surface colonization (new cells adhering to attached dead cells), as evidenced by the high rates of biofilm-related disease that persist globally [4, 39]. Since Psl adsorption plays a key role in the mechanism of *P. aeruginosa* cell attachment and biofilm formation, our approach specifically targets and disrupts this microbial adhesion mechanism. This approach differs from non-specific mechanisms to non-fouling such as SLIPS (slippery liquid infused porous surfaces) [61–62], and other non-wetting surfaces. For well-known, common pathogens it seems advantageous to target cell attachment, at the early stages of biofilm development. It has also been reported that, in mixed species biofilms, Psl can also contribute to the protection of other pathogens such as *Escherichia coli* and *Staphylococcus aureus* from antimicrobials[15]. Therefore, specific, selective prevention of *P. aeruginosa* biofilm formation should not only help enable antibiotic therapies to eradicate infections and reduce the development of acquired resistance, but also help the host immune system to eliminate infections associated with medical devices that are caused by both biofilm and non-biofilm producers.

The immobilization of the $PslG_h$ glycoside hydrolase uniformly along the full length of these medical grade, small-diameter PE catheters, has been a significant technical achievement due to the inert nature of PE, and the physically confinement of access to the lumen surface (inside a 1mm tube, 14 cm long) for the plasma and solution penetration. The lumen surface of implanted catheters can become exposed to blood and body fluids, and has a high risk of biofilm infection. Previous efforts to functionalize catheter lumen surfaces, such as uniform activation with polar groups, was shown to be a challenge [63]. The narrow PE-100 catheters used herein thus represent a kind of ‘worst case’ application for medical devices, and our results suggest that a wide range of device sizes, material types and morphologies should be possible for enzyme immobilization.

A key finding in our work here is *stability*. The results show a consistent, stable activity of these enzymes to disrupt biofilm formation (through continuous Psl polysaccharide degradation) under *in vitro* flow conditions for extended periods (14 d), after extensive sterilization and storage (30 d, 4°C), and in the complexity of an *in vivo* environment. These results suggest that $PslG_h$ remains active after surface immobilization, which may make them suitable for a wide range of medical devices. Importantly, the immobilization procedure helped to maintain sterility of the catheters as conventional methods such as ethylene oxide did not work as the sterilized $PslG_h$ surfaces lost their anti-biofilm activity (Figure S5). The difference between the CFU log reduction observed *in vivo* (Figure 7B)

and that observed in the *in vitro* assay (Figure 6B) likely reflects the enhanced biofilm formation capacity of strain ATCC 27853 [59] as well as the effect body fluids and blood serum on promoting the biofilm growth [64]. Overall, our work demonstrates that covalent immobilization of enzymes on biomedical tubing surfaces can represent an effective and feasible design strategy for non-fouling antimicrobial material design. These represent a 'bio-active' interface to specifically prevent bacterial adhesion mechanisms through continuous hydrolytic activity of a biofilm matrix component.

5. Conclusions

In summary, we have generated a sterile, uniform, and high-density surface of immobilized $PslG_h$ enzyme throughout the lumen of long, small diameter, medical grade catheters, in an effort to improve the performance of indwelling catheters against microbial biofilm growth. The catheters were highly effective at preventing *P. aeruginosa* biofilm growth under both static and dynamic flow conditions *in vitro*, and even for long periods of time (11 days). Finally, preliminary *in vivo* results show the $PslG_h$-bound catheters dramatic resistance to biofilm growth in the complex environment of an infection model. These results demonstrate for the first time that 'bio-active' enzyme-modification of surfaces can realistically be applied to a wide range of biomaterials, uniformly over large areas, and with long-term activity. There is a wide range of biomedical devices that may benefit from these effects on *P. aeruginosa* biofilm growth, to significantly impact the problem of hospital acquired infections, complications and costs [54].

Supplementary Material

Refer to Web version on PubMed Central for supplementary material.

References

1. Costerton J; Stewart PS; Greenberg E, Bacterial biofilms: a common cause of persistent infections. Science 1999, 284 (5418), 1318–1322. [PubMed: 10334980]
2. Del Pozo J; Patel R, The challenge of treating biofilm-associated bacterial infections. Clinical Pharmacology & Therapeutics 2007, 82 (2), 204–209. [PubMed: 17538551]
3. Percival SL; Suleman L; Vuotto C; Donelli G, Healthcare-associated infections, medical devices and biofilms: risk, tolerance and control. Journal of medical microbiology 2015, 64 (4), 323–334. [PubMed: 25670813]
4. Wolcott R; Rhoads D; Bennett M; Wolcott B; Gogokhia L; Costerton J; Dowd S, Chronic wounds and the medical biofilm paradigm. Journal of wound care 2010, 19 (2), 45–53. [PubMed: 20216488]
5. Flemming H-C; Wingender J, The biofilm matrix. Nature Reviews Microbiology 2010, 8 (9), 623. [PubMed: 20676145]
6. Richards MJ; Edwards JR; Culver DH; Gaynes RP, Nosocomial infections in medical intensive care units in the United States. National Nosocomial Infections Surveillance System. Critical care medicine 1999, 27 (5), 887–892. [PubMed: 10362409]
7. Ryder MA, Catheter-related infections: it's all about biofilm. Topics in Advanced Practice Nursing eJournal 2005, 5 (3), 2005.
8. Zimlichman E; Henderson D; Tamir O; Franz C; Song P; Yamin CK; Keohane C; Denham CR; Bates DW, Health care–associated infections: a meta-analysis of costs and financial impact on the US health care system. JAMA internal medicine 2013, 173 (22), 2039–2046. [PubMed: 23999949]
9. Mermel LA; Allon M; Bouza E; Craven DE; Flynn P; O'Grady NP; Raad II; Rijnders BJ; Sherertz RJ; Warren DK, Clinical practice guidelines for the diagnosis and management of intravascular

catheter-related infection: 2009 Update by the Infectious Diseases Society of America. Clinical infectious diseases 2009, 49 (1), 1–45. [PubMed: 19489710]

10. Hall-Stoodley L; Costerton JW; Stoodley P, Bacterial biofilms: from the natural environment to infectious diseases. Nature Reviews Microbiology 2004, 2 (2), 95–108. [PubMed: 15040259]
11. Reid G, Biofilms in infectious disease and on medical devices. International journal of antimicrobial agents 1999, 11 (3), 223–226. [PubMed: 10394974]
12. Loo C-Y; Lee W-H; Young PM; Cavaliere R; Whitchurch CB; Rohanizadeh R, Implications and emerging control strategies for ventilator-associated infections. Expert Review of Anti-infective Therapy 2015, 13, 379–393. [PubMed: 25632800]
13. Campoccia D; Montanaro L; Arciola CR, A review of the biomaterials technologies for infection-resistant surfaces. Biomaterials 2013, 34 (34), 8533–8554. [PubMed: 23953781]
14. Colvin KM; Gordon VD; Murakami K; Borlee BR; Wozniak DJ; Wong GC; Parsek MR, The pel polysaccharide can serve a structural and protective role in the biofilm matrix of Pseudomonas aeruginosa. PLoS pathogens 2011, 7 (1), e1001264. [PubMed: 21298031]
15. Billings N; Millan MR; Caldara M; Rusconi R; Tarasova Y; Stocker R; Ribbeck K, The extracellular matrix component Psl provides fast-acting antibiotic defense in Pseudomonas aeruginosa biofilms. PLoS pathogens 2013, 9 (8), e1003526. [PubMed: 23950711]
16. Mishra M; Byrd MS; Sergeant S; Azad AK; Parsek MR; McPhail L; Schlesinger LS; Wozniak DJ, Pseudomonas aeruginosa Psl polysaccharide reduces neutrophil phagocytosis and the oxidative response by limiting complement-mediated opsonization. Cellular microbiology 2012, 14 (1), 95–106. [PubMed: 21951860]
17. Alhede M; Bjarnsholt T; Givskov M, Pseudomonas aeruginosa biofilms: mechanisms of immune evasion. Adv Appl Microbiol 2014, 86, 1–40. [PubMed: 24377853]
18. Davies D, Understanding biofilm resistance to antibacterial agents. Nature reviews Drug discovery 2003, 2 (2), 114–122. [PubMed: 12563302]
19. Høiby N; Ciofu O; Johansen HK; Song Z.-j.; Moser C; Jensen PØ; Molin S; Givskov M; Tolker-Nielsen T; Bjarnsholt T, The clinical impact of bacterial biofilms. International journal of oral science 2011, 3 (2), 55. [PubMed: 21485309]
20. Barnes L; Cooper I, Biomaterials and Medical Device-Associated Infections. Elsevier: 2014.
21. Phillips KS; Patwardhan D; Jayan G, Biofilms, medical devices, and antibiofilm technology: Key messages from a recent public workshop. American journal of infection control 2015, 43 (1), 2. [PubMed: 25448303]
22. Treter J; Macedo A, Catheters: a suitable surface for biofilm formation. Handbook: science against microbial pathogens: communicating current research and technological advances. Spain: Formatex Research Center 2011, 835–842.
23. Giesecke MT; Schwabe P; Wichlas F; Trampuz A; Kleber C, Impact of high prevalence of pseudomonas and polymicrobial gram-negative infections in major sub-/total traumatic amputations on empiric antimicrobial therapy: a retrospective study. World J Emerg Surg 2014, 9 (1), 55. [PubMed: 25364376]
24. Ciofu O; Tolker-Nielsen T, Tolerance and Resistance of Pseudomonas aeruginosa Biofilms to Antimicrobial Agents—How P. aeruginosa Can Escape Antibiotics. Frontiers in Microbiology 2019, 10 (913).
25. Livermore DM, Multiple mechanisms of antimicrobial resistance in Pseudomonas aeruginosa: our worst nightmare? Clinical infectious diseases 2002, 34 (5), 634–640. [PubMed: 11823954]
26. Kang C-I; Kim S-H; Kim H-B; Park S-W; Choe Y-J; Oh M.-d.; Kim E-C; Choe K-W, Pseudomonas aeruginosa bacteremia: risk factors for mortality and influence of delayed receipt of effective antimicrobial therapy on clinical outcome. Clinical infectious diseases 2003, 37 (6), 745–751. [PubMed: 12955633]
27. Khan W; Bernier SP; Kuchma SL; Hammond JH; Hasan F; O'Toole GA, Aminoglycoside resistance of Pseudomonas aeruginosa biofilms modulated by extracellular polysaccharide. International microbiology: the official journal of the Spanish Society for Microbiology 2010, 13 (4), 207. [PubMed: 21404215]
28. Zegans ME; Wozniak D; Griffin E; Toutain-Kidd CM; Hammond JH; Garfoot A; Lam JS, Pseudomonas aeruginosa exopolysaccharide Psl promotes resistance to the biofilm inhibitor

polysorbate 80. Antimicrobial agents and chemotherapy 2012, 56 (8), 4112–4122. [PubMed: 22585230]

29. Bjarnsholt T; Jensen PØ; Fiandaca MJ; Pedersen J; Hansen CR; Andersen CB; Pressler T; Givskov M; Høiby N, Pseudomonas aeruginosa biofilms in the respiratory tract of cystic fibrosis patients. Pediatric pulmonology 2009, 44 (6), 547–558. [PubMed: 19418571]
30. Deschaght P; De Baere T; Van Simaey L; De Baets F; De Vos D; Pirnay J-P; Vaneechoutte M, Comparison of the sensitivity of culture, PCR and quantitative real-time PCR for the detection of Pseudomonas aeruginosa in sputum of cystic fibrosis patients. BMC microbiology 2009, 9 (1), 1. [PubMed: 19121223]
31. Schmidt KD; Tümmler B; Römling U, Comparative genome mapping of Pseudomonas aeruginosa PAO with P. aeruginosa C, which belongs to a major clone in cystic fibrosis patients and aquatic habitats. Journal of bacteriology 1996, 178 (1), 85–93. [PubMed: 8550447]
32. Colvin KM; Irie Y; Tart CS; Urbano R; Whitney JC; Ryder C; Howell PL; Wozniak DJ; Parsek MR, The Pel and Psl polysaccharides provide Pseudomonas aeruginosa structural redundancy within the biofilm matrix. Environmental microbiology 2012, 14 (8), 1913–1928. [PubMed: 22176658]
33. Ma L; Wang J; Wang S; Anderson EM; Lam JS; Parsek MR; Wozniak DJ, Synthesis of multiple Pseudomonas aeruginosa biofilm matrix exopolysaccharides is post-transcriptionally regulated. Environmental microbiology 2012, 14 (8), 1995–2005. [PubMed: 22513190]
34. Ma L; Conover M; Lu H; Parsek MR; Bayles K; Wozniak DJ, Assembly and development of the Pseudomonas aeruginosa biofilm matrix. PLoS pathogens 2009, 5 (3), e1000354. [PubMed: 19325879]
35. Zhao K; Tseng BS; Beckerman B; Jin F; Gibiansky ML; Harrison JJ; Luijten E; Parsek MR; Wong GC, Psl trails guide exploration and microcolony formation in Pseudomonas aeruginosa biofilms. Nature 2013, 497 (7449), 388–391. [PubMed: 23657259]
36. Zilberman M; Elsner JJ, Antibiotic-eluting medical devices for various applications. J Control Release 2008, 130 (3), 202–15. [PubMed: 18687500]
37. Donelli G; Francolini I, Efficacy of antiadhesive, antibiotic and antiseptic coatings in preventing catheter-related infections: review. J Chemother 2001, 13 (6), 595–606. [PubMed: 11806619]
38. Kluin OS; van der Mei HC; Busscher HJ; Neut D, A surface-eroding antibiotic delivery system based on poly-(trimethylene carbonate). Biomaterials 2009, 30 (27), 4738–4742. [PubMed: 19500839]
39. Koo H; Allan RN; Howlin RP; Stoodley P; Hall-Stoodley L, Targeting microbial biofilms: current and prospective therapeutic strategies. Nature Reviews Microbiology 2017, 15 (12), 740. [PubMed: 28944770]
40. Ostendorf T; Meinhold A; Harter C; Salwender H; Egerer G; Geiss HK; Ho AD; Goldschmidt H, Chlorhexidine and silver-sulfadiazine coated central venous catheters in haematological patients—a double-blind, randomised, prospective, controlled trial. Supportive care in cancer 2005, 13 (12), 993–1000. [PubMed: 15834740]
41. Bridges K; Kidson A; Lowbury E; Wilkins M, Gentamicin-and silver-resistant pseudomonas in a burns unit. BMJ 1979, 1 (6161), 446–449. [PubMed: 106914]
42. Percival S; Bowler P; Russell D, Bacterial resistance to silver in wound care. Journal of hospital infection 2005, 60 (1), 1–7.
43. Chen M; Yu Q; Sun H, Novel strategies for the prevention and treatment of biofilm related infections. International journal of molecular sciences 2013, 14 (9), 18488–18501. [PubMed: 24018891]
44. Bazaka K; Jacob MV; Crawford RJ; Ivanova EP, Efficient surface modification of biomaterial to prevent biofilm formation and the attachment of microorganisms. Applied microbiology and biotechnology 2012, 95 (2), 299–311. [PubMed: 22618687]
45. Salwiczek M; Qu Y; Gardiner J; Strugnell RA; Lithgow T; McLean KM; Thissen H, Emerging rules for effective antimicrobial coatings. Trends in biotechnology 2014, 32 (2), 82–90. [PubMed: 24176168]
46. Harris JM, Poly (ethylene glycol) chemistry: biotechnical and biomedical applications. Springer Science & Business Media: 2013.

47. Michel R; Pasche S; Textor M; Castner DG, Influence of PEG architecture on protein adsorption and conformation. Langmuir 2005, 21 (26), 12327–12332. [PubMed: 16343010]
48. Wong T-S; Kang SH; Tang SK; Smythe EJ; Hatton BD; Grinthal A; Aizenberg J, Bioinspired self-repairing slippery surfaces with pressure-stable omniphobicity. Nature 2011, 477 (7365), 443–447. [PubMed: 21938066]
49. Baker P; HIll PJ; Snarr BD; Alnabelseya N; Pestrak MJ; Lee MJ; Jennings LK; Tam J; Melnyk RA; Parsek MR, Exopolysaccharide biosynthetic glycoside hydrolases can be utilized to disrupt and prevent Pseudomonas aeruginosa biofilms. Science Advances 2016, 2 (5), e1501632. [PubMed: 27386527]
50. Baker P; Whitfield GB; Hill PJ; Little DJ; Pestrak MJ; Robinson H; Wozniak DJ; Howell PL, Characterization of the Pseudomonas aeruginosa Glycoside Hydrolase PslG Reveals That Its Levels Are Critical for Psl Polysaccharide Biosynthesis and Biofilm Formation. J Biol Chem 2015, 290 (47), 28374–87. [PubMed: 26424791]
51. Asker D; Awad TS; Baker P; Howell PL; Hatton BD, Non-eluting, surface-bound enzymes disrupt surface attachment of bacteria by continuous biofilm polysaccharide degradation. Biomaterials 2018, 167, 168–176. [PubMed: 29571052]
52. Pestrak MJ; Baker P; Dellos-Nolan S; Hill PJ; Passos da Silva D; Silver H; Lacdao I; Raju D; Parsek MR; Wozniak DJ; Howell PL, Treatment with the Pseudomonas aeruginosa Glycoside Hydrolase PslG Combats Wound Infection by Improving Antibiotic Efficacy and Host Innate Immune Activity. Antimicrobial Agents and Chemotherapy 2019, 63 (6), e00234–19. [PubMed: 30988141]
53. Buthe A; Wu S; Wang P, Nanoporous silica glass for the immobilization of interactive enzyme systems. Enzyme Stabilization and Immobilization: Methods and Protocols 2011, 37–48.
54. Rasband WS, ImageJ. U. S. National Institutes of Health; Bethesda, Maryland, USA: 1997–2008. http://rsb.info.nih.gov/ij/.
55. Brugnara M, Contact Angle Plugin. University of Trento, Trento, Italy 2010.
56. Andes D; Nett J; Oschel P; Albrecht R; Marchillo K; Pitula A, Development and characterization of an in vivo central venous catheter Candida albicans biofilm model. Infection and immunity 2004, 72 (10), 6023–6031. [PubMed: 15385506]
57. Gutowski W; Wu DY; Li S, Surface silanization of polyethylene for enhanced adhesion. The Journal of Adhesion 1993, 43 (1–2), 139–155.
58. Onyshchenko I; De Geyter N; Nikiforov AY; Morent R, Atmospheric pressure plasma penetration inside flexible polymeric tubes. Plasma Processes and Polymers 2015, 12 (3), 271–284.
59. Cao H; Lai Y; Bougouffa S; Xu Z; Yan A, Comparative genome and transcriptome analysis reveals distinctive surface characteristics and unique physiological potentials of Pseudomonas aeruginosa ATCC 27853. BMC Genomics 2017, 18 (1), 459. [PubMed: 28606056]
60. Hatton BD, 13 - Antimicrobial coatings for metallic biomaterials. In Surface Coating and Modification of Metallic Biomaterials, Wen C, Ed. Woodhead Publishing: 2015; pp 379–391.
61. Lavielle N; Asker D; Hatton BD, Lubrication dynamics of swollen silicones to limit long term fouling and microbial biofilms. Soft Matter 2021, 17 (4), 936–946. [PubMed: 33284301]
62. Awad TS; Asker D; Hatton BD, Food-Safe Modification of Stainless Steel Food-Processing Surfaces to Reduce Bacterial Biofilms. ACS Applied Materials & Interfaces 2018, 10 (27), 22902–22912. [PubMed: 29888590]
63. Zhou C; Wu Y; Thappeta KRV; Subramanian JTL; Pranantyo D; Kang E-T; Duan H; Kline K; Chan-Park MB, In vivo anti-biofilm and anti-bacterial non-leachable coating thermally polymerized on cylindrical catheter. ACS applied materials & interfaces 2017, 9 (41), 36269–36280. [PubMed: 28945343]
64. Batoni G; Maisetta G; Esin S, Antimicrobial peptides and their interaction with biofilms of medically relevant bacteria. Biochimica et Biophysica Acta (BBA)-Biomembranes 2016, 1858 (5), 1044–1060. [PubMed: 26525663]

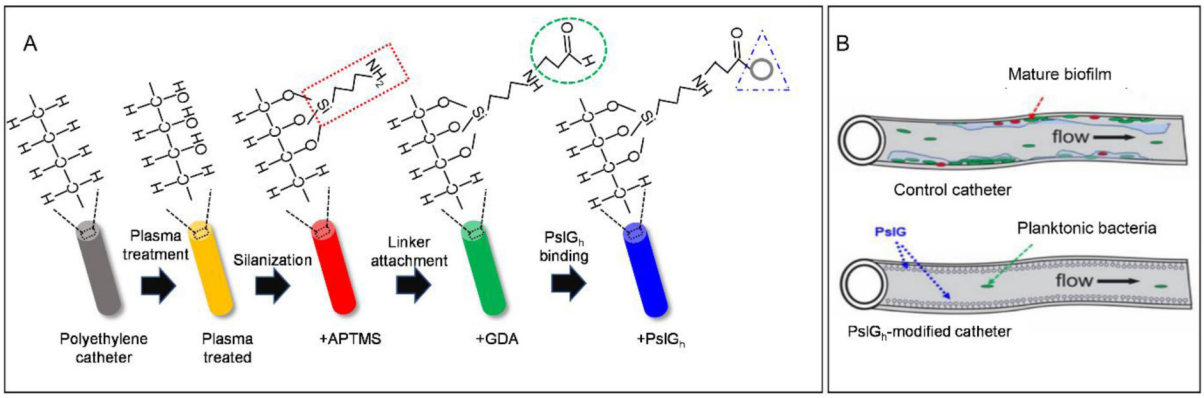

Figure 1.

(A) Schematic illustration of the sequence of steps involved in enzyme immobilization: surface activation by plasma treatment; amine (NH2) functionalization with 3-aminopropyltrimethoxysilane (APTMS) via silanization; activation of the catheter lumen surface using the bifunctional agent (GDA) under the formation of Schiff base and finally coupling of the enzyme. (B) Chemical immobilization of $PslG_h$ prevents *P. aeruginosa* biofilm formation on the luminal surface of catheter tubing. Schematic representation demonstrating cell attachment and biofilm formation on untreated catheters (top) and inhibition of biofilm formation when the catheter is treated with $PslG_h$ (bottom).

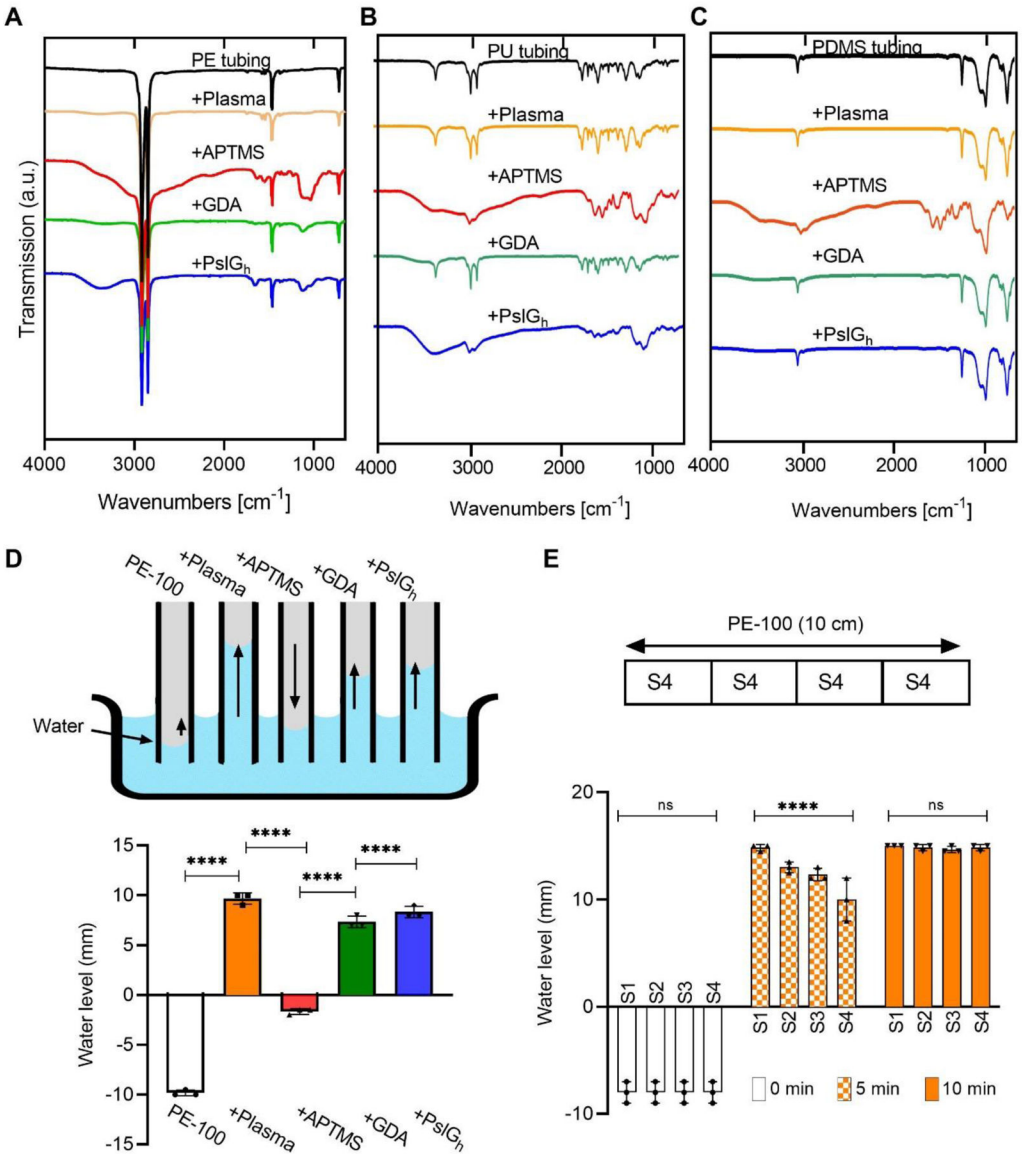

Figure 2.

Chemical and physical characterization of the lumen of commercial polymer tubing and a medical grade catheter. (A-C) ATR-FTIR spectra showing the surface chemical groups lining the PE, PU and PDMS tubing lumen during immobilization; (D) Variation in the relative water level inside PE tubing after each immobilization step. A rise in the water level within catheter lumen is indicative of hydrophilic character; and (E) Relative displacement of water inside 4 lumen segments (S1-S4) of a 10cm long PE-100 catheter after treatment with atmospheric plasma for 10 min. ****P ≤ 0.0001. NS, no significant difference.

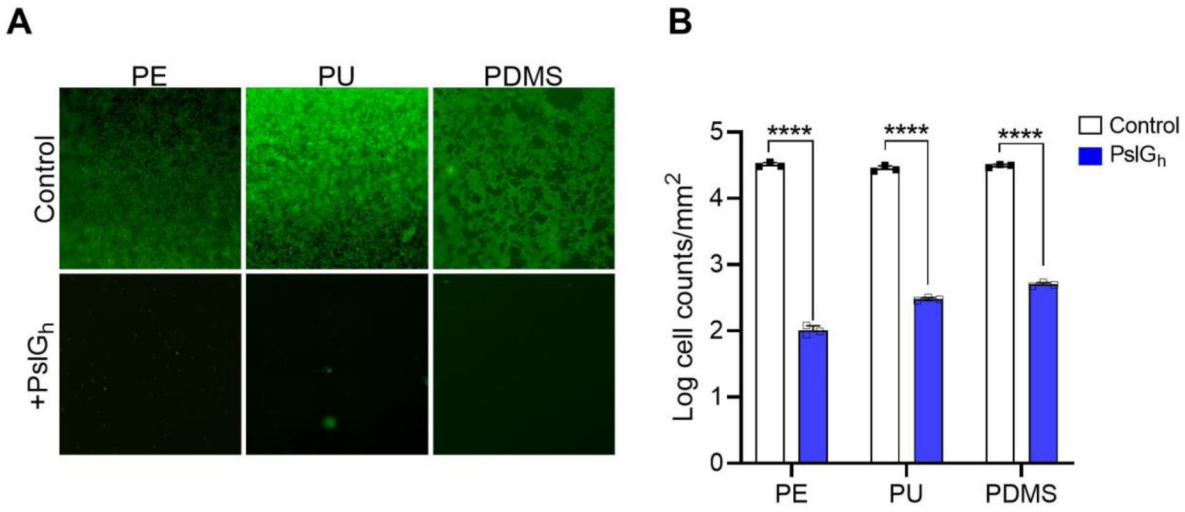

Figure 3.

Bound PslG$_h$ prevents *P. aeruginosa* biofilm formation on the luminal surface of polymer tubing. (A) Florescence images showing the inhibition of biofilm formation by bound PslG$_h$ on the luminal surface of PE, PU and PDMS tubing, but not for the untreated control. (B) Corresponding cell counts (per cm^2) calculated from the image analysis of surfaces in (A). ****P ≤ 0.0001.

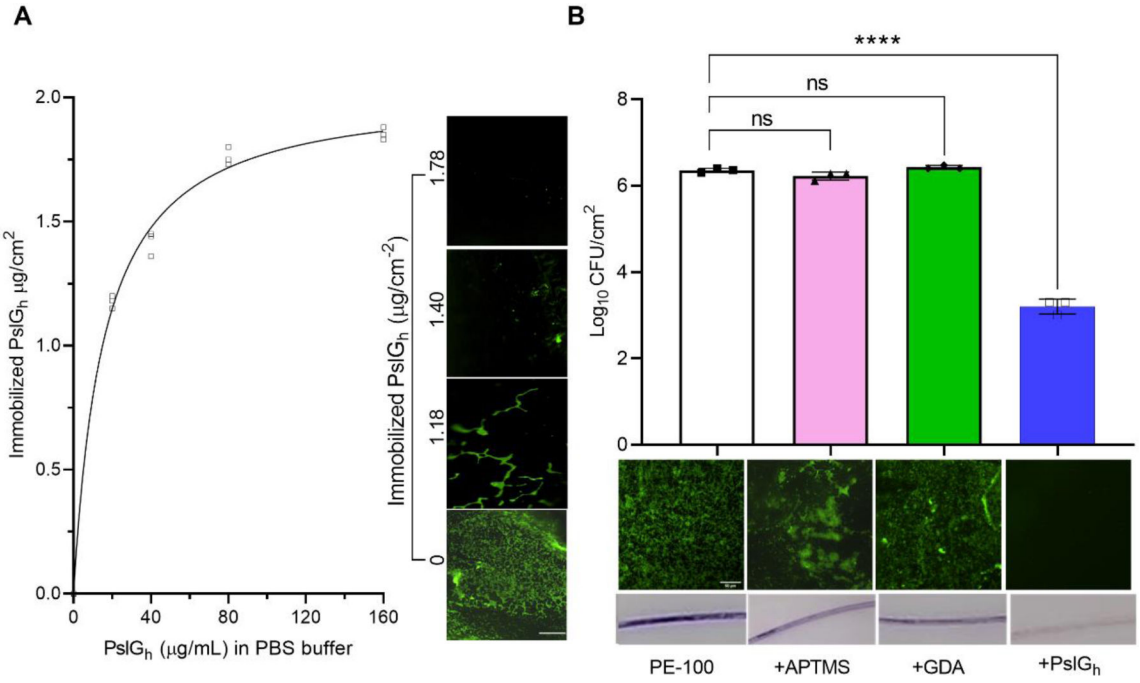

Figure 4.

PslG$_h$-modified PE-100 catheter inhibits biofilm formation (A) Effective concentration of immobilized PslG$_h$ required for biofilm inhibition. Effect of PslG$_h$ concentration (µg/mL) in immobilization solution on its binding capacity to catheter luminal surface (µg/cm) (left). Effect of immobilized PslG$_h$ surface density on biofilm formation of *Pseudomonas aeruginosa* PAO1 (right). (B) Anti-biofilm activity of the PE catheter lumen with bound PslG$_h$, relative to the untreated control, or APTMS and GDA functionalized surfaces. (A) Colony forming units per cm^2 (CFU) (top), corresponding florescence images (middle), and crystal violet (CV) stained images (bottom). All measurements were acquired after incubation for 24 h in bacterial culture. Biofilms were stained with SYTOX Green (middle) and CV (bottom) (scale bar, 50 µm). ****P ≤ 0.001. NS, no significant difference.

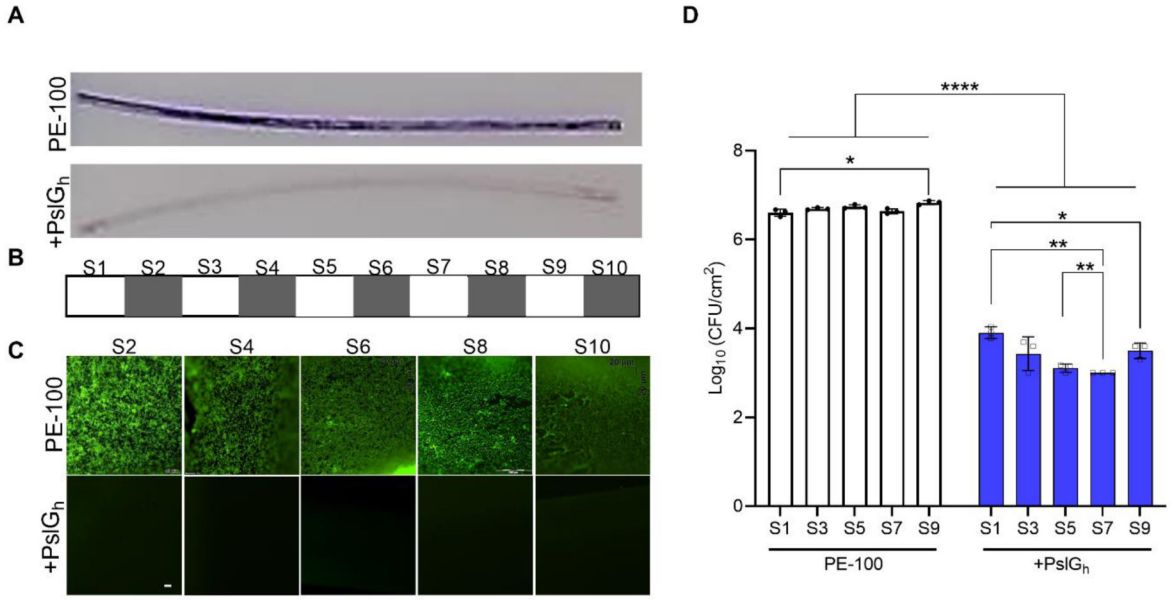

Figure 5.

Antibiofilm activity of the lumen of high density PslG$_h$-bound 10 cm PE-100 catheters against *P. aeruginosa*. (A) Photos of CV stained 10 cm PE-100 catheters; (B) Fluorescence images of 5 alternating segments (i.e., S2, 4, 6, 8 and 10); and (C) Colony forming units per cm^2 (CFU) of the other 5 alternating segments (i.e., S1, 3, 5, 7 and 9). All measurements were acquired after incubation for 24 h in bacterial culture. Biofilms were stained with CV in (A) and with SYTOX Green in (B) (scale bar, 50 μm). *P ≤ 0.05, **P ≤ 0.01, ****P ≤ 0.0001.

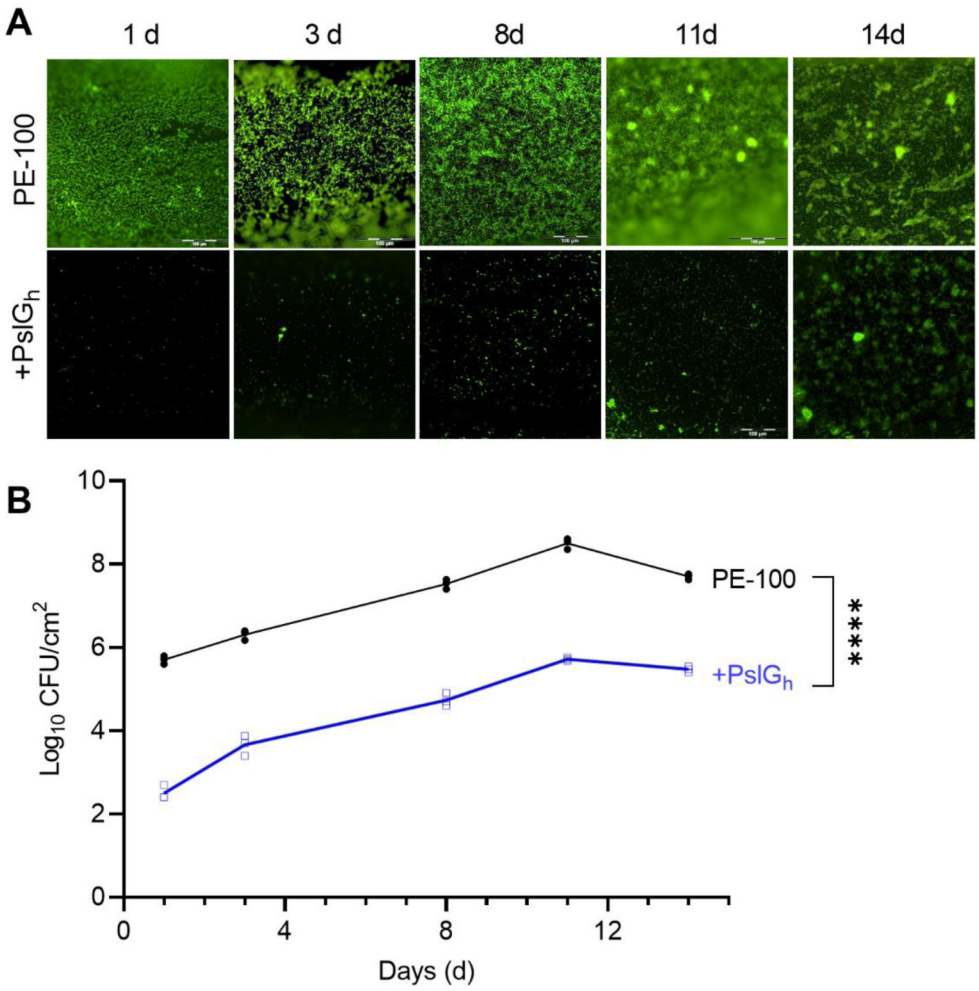

Figure 6.

Inhibition of *P. aeruginosa* biofilm formation by $PslG_h$ bound to the lumen surface of PE-100 catheter under dynamic flow culture conditions. (A) Fluorescence images of biofilm growth for up to 14 days on the lumen surface of untreated (top) and $PslG_h$-bound PE-100 catheter (bottom). (B) Colony forming units (CFU/cm^2) of *P. aeruginosa* PAO1 on the lumen surface of untreated and $PslG_h$-bound PE-100 catheter after 14 d incubation. Biofilms were stained with SYTOX Green in (A) (scale bar, 100 μm). ****$P \leq 0.0001$.

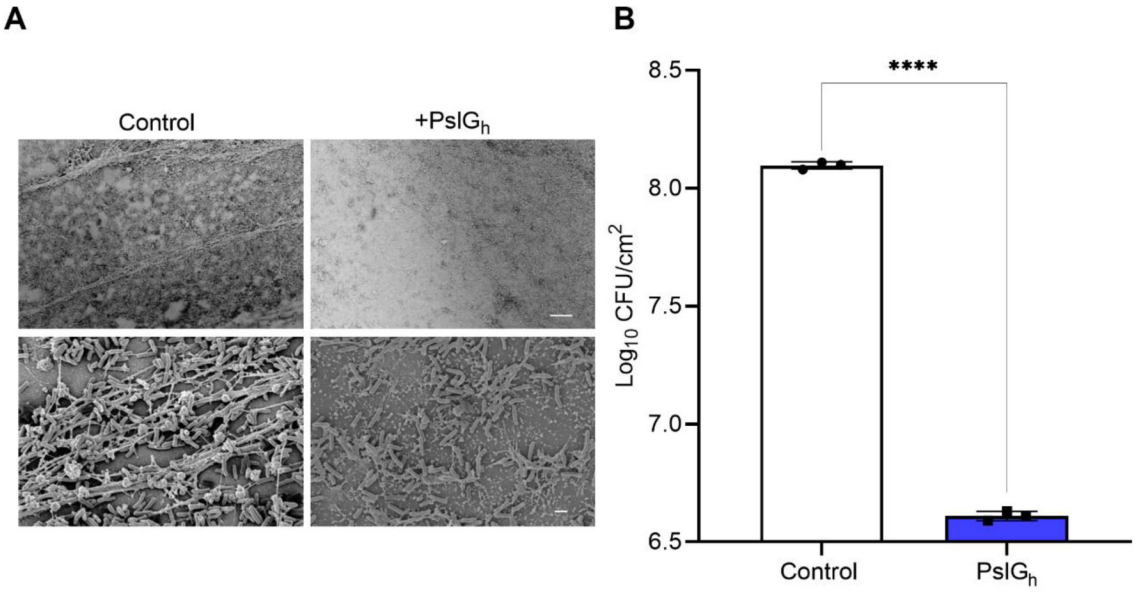

Figure 7.

In vivo inhibition of biofilm formation of *P. aeruginosa* ATCC 27853 on the PslG$_h$-treated lumen surface of PE catheter. (A) SEM images of biofilm growth on untreated and treated PE-100 catheters at low magnification (1,000X), and (B) corresponding bacterial burden showing ~ 2 log CFU /cm^2 reduction in *P. aeruginosa* ATCC 27853 cells after 1d of placement *in vivo*. The scale bars represent 20 μm, respectively. ****P ≤ 0.0001.